Intravascular large B-cell lymphoma mimicking an orbital mass lesion and bilateral cavernous sinus syndrome: A case report

QIONG WU[1], YIRAN JIA[1], BENTAO YANG[2], XIAOJIN HE[3], HONGJUAN LIU[1] and LIBIN JIANG[1]

[1]Beijing Tongren Eye Center, Beijing Tongren Hospital, Capital Medical University, Beijing Ophthalmology and Visual Sciences Key Laboratory, Beijing 100730, P.R. China; [2]Department of Radiology, Beijing Tongren Hospital, Capital Medical University, Beijing 100730, P.R. China; [3]Department of Pathology, Beijing Tongren Hospital, Capital Medical University, Beijing 100730, P.R. China

Received August 26, 2025; Accepted March 10, 2026

DOI: 10.3892/ol.2026.15584

Abstract. Intravascular large B-cell lymphoma (IVLBCL) is a rare entity that can present with atypical extranodal manifestations, often mimicking other orbital or neurological conditions. A 69-year-old woman presented with rapidly progressive left ptosis and diplopia, which progressed to complete bilateral ophthalmoplegia within several weeks. Magnetic resonance imaging revealed a previously unreported right orbital mass accompanied by bilateral cavernous sinus (CS) enhancement, representing a novel imaging feature of IVLBCL. The diagnosis was established by sphenoid sinus biopsy. The patient achieved near-clinical remission, with almost complete resolution of the orbital mass, following rituximab, cyclophosphamide, doxorubicin, vincristine and prednisolone (R-CHOP) chemotherapy combined with a Bruton tyrosine kinase inhibitor and intravenous high-dose methotrexate. However, diplopia recurred at 3 months post-treatment, indicating that although the patient initially responded well to R-CHOP-based combination therapy, more effective maintenance or consolidation strategies should be actively explored for patients with IVLBCL involving the central nervous system. Clinically, various lymphoma subtypes should be considered in the differential diagnosis of patients presenting with CS and intraorbital lesions.

Introduction

Intravascular large B-cell lymphoma (IVLBCL) is a rare and aggressive subtype of diffuse LBCL (DLBCL) characterized by non-specific clinical manifestations, which frequently lead to a delayed diagnosis. The incidence of IVLBCL is extremely low, occurring in fewer than 0.5 cases per million people, with a median age at diagnosis of 70 years, and the 5-year overall survival was 46.4% (1,2). Central nervous system (CNS) involvement occurs in 30-40% of cases and typically manifests as neurological deficits secondary to cerebral circulatory impairment, making it the second most common presentation of IVLBCL (3). Cavernous sinus syndrome (CSS) is defined by dysfunction of cranial nerves III, IV, V and VI, manifesting as ptosis, diplopia, ophthalmoplegia and facial sensory loss, with etiologies ranging from tumors to inflammatory conditions (4). The overlap between IVLBCL-related CSS and other orbital pathologies creates significant diagnostic challenges, as radiological findings may mimic orbital masses (5,6). To the best of our knowledge, for the first time, the present study reports an IVLBCL case presenting as bilateral CS syndrome with diplopia, ptosis and a right orbital mass. This study aims to highlight the rare presentation of IVLBCL as bilateral CS syndrome, emphasize the diagnostic challenges of its orbital and neurological manifestations and underscore the critical role of early tissue biopsy in diagnosis.

Case report

A 69-year-old woman presented in November 2023 with binocular diplopia 3 days after the onset of a fever. The patient was evaluated at the Ophthalmology Clinic of Beijing Tongren Hospital, Capital Medical University (Beijing, China). In 2020, the patient had been diagnosed with hypertension, and their blood pressure had since been controlled on a combination of valsartan (80 mg/day) and amlodipine (10 mg/day). The patient also had a 4-year history of type 2 diabetes mellitus and was taking oral empagliflozin (25 mg/day); however, suboptimal glycemic control was being achieved, with an elevated hemoglobin A1c level at 7.5% (normal range: 4-6%). The patient had a past history of coronary artery disease for which isosorbide dinitrate 10 mg 3 times daily was being prescribed. Best-corrected visual acuity was 20/60 in both the right [oculus dexter (OD)] and left [oculus sinister (OS)] eyes, and intraocular pressures were within normal limits. Bilateral nuclear cataracts (grade 2) were present, while funduscopic examination was unremarkable. The OD exhibited normal

Correspondence to: Professor Libin Jiang, Beijing Tongren Eye Center, Beijing Tongren Hospital, Capital Medical University, Beijing Ophthalmology and Visual Sciences Key Laboratory, 1 Dongjiaominxiang Street, Dongcheng, Beijing 100730, P.R. China
E-mail: 13693664088@163.com

Key words: intravascular large B-cell lymphoma, cavernous sinus syndrome, orbit, diplopia, ptosis

ocular motility, with a 3-mm pupil reactive to light. By contrast, the OS showed ptosis, with the upper eyelid margin at the mid-pupillary level, complete ophthalmoplegia and a fixed mydriasis measuring 6 mm. Neurological assessment revealed isolated hypoesthesia in the left frontal dermatome. Blood tests showed normal red blood cell, white blood cell and platelet counts, but elevated levels of fibrinogen degradation product (5.8 μg/ml; normal range: 0-5 μg/ml), D-dimer (2.33 mg/l; normal range: 0-0.55 mg/l) and lactate dehydrogenase (461 U/l; normal range: 120-250 U/l). A peripheral blood smear was evaluated and showed no abnormalities.

Routine cerebrospinal fluid (CSF) tests and biochemical indices were normal. CSF analyses, including ink staining, Gram staining, acid-fast staining, and bacterial and fungal cultures, were all negative. CSF pressure was 105 mm H_2O (80-180 mmH_2O), and no tumor cells were identified on CSF pathological examination. Orbital MRI revealed a 15.9x5.9 mm lesion at the right orbital apex, while contrast-enhanced MRI showed abnormal thickening and enhancement of bilateral CSs, extending to the adjacent dura mater and clivus (Fig. 1A). A CT scan of the skull base, orbit and sinuses showed no bony destruction and adjacent hyperostosis (Fig. 1B and C). An idiopathic orbital inflammatory pseudotumor was initially suspected, and intravenous methylprednisolone pulse therapy was initiated (120 mg on days 1-3 and 80 mg on days 4-6) but was discontinued due to severe gastrointestinal symptoms. The ptosis and complete external ophthalmoplegia of the left eye showed no improvement. Over the subsequent week, the patient developed complete bilateral external ophthalmoplegia, severe bilateral blepharoptosis completely covering the pupils, and bilateral fixed and dilated pupils (OD, 5 mm; OS, 6mm). Follow-up MRI revealed multifocal abnormal enhancement in multiple areas, including the bilateral CSs, right orbital compartment, sinonasal cavities, clivus and marrow cavity of the left pterygoid process (Fig. 1D-H).

Subsequently, a transnasal endoscopic sphenoid sinus biopsy was performed, leading to a definitive diagnosis of IVLBCL. Histopathological examination was performed on the sphenoid sinus biopsy specimens. For histopathological analysis, the specimens were fixed in 4% neutral formalin (Beijing Yili Fine Chemical Co., Ltd.) at room temperature for 24 h, embedded in paraffin and sectioned at a thickness of 4 μm. Hematoxylin and eosin (H&E) staining was performed at room temperature (5 min for hematoxylin, 3 min for eosin) using reagents from Beijing Yili Fine Chemical Co., Ltd. Examination with a Nikon ECLIPSE Ci Series Upright Clinical Microscope (Nippon Kogaku) revealed neoplastic lymphocytes proliferating within vascular lumina, with round to oval nuclei, coarse chromatin and prominent nucleoli (x100, x400 magnification). Immunohistochemical analysis was performed using the Dako EnVision System (Agilent Technologies, Inc.). Endogenous peroxidase was blocked with 3% hydrogen peroxide at room temperature for 10 min (no serum blocking reagent was used). All primary antibodies were mouse monoclonal anti-human, purchased from Beijing Zhongshan Golden Bridge Biotechnology Co., Ltd. (OriGene Technologies, Inc.), diluted in PBS and incubated at 25˚C for 30 min. The primary antibodies used included: CD20 (cat. no. ZM-0036; dilution 1:150), CD19 (cat. no. ZM-0027; dilution 1:100), CD79α (cat. no. ZM-0028; dilution 1:100), multiple myeloma oncogene 1 (MUM1; cat. no. ZA-0511; dilution 1:150), B-cell lymphoma 2 (BCL-2; cat. no. ZM-0024; dilution 1:100), leukocyte common antigen (LCA/CD45; cat. no. ZM-0039; dilution 1:150), CD5 (cat. no. ZM-0037; dilution 1:150), CD3 (cat. no. ZM-0062; dilution 1:150), CD10 (cat. no. ZM-0048; dilution 1:100), CD23 (cat. no. ZM-0050; dilution 1:100), BCL-6 (cat. no. ZA-0512; dilution 1:150), terminal deoxynucleotidyl transferase (TdT; cat. no. ZA-0513; dilution 1:100), CyclinD1 (cat. no. ZA-0514; dilution 1:150), CD34 (cat. no. ZM-0046; dilution 1:150), Ki-67 (cat. no. ZA-0502; dilution 1:150), CD61 (cat. no. ZM-0063; dilution 1:100), myeloperoxidase (MPO; cat. no. ZM-0064; dilution 1:150), CD3 (cat. no. ZM-0062; dilution 1:150) and CD117 (cat. no. ZM-0437; dilution 1:100). The secondary antibody was horseradish peroxidase-conjugated, provided in the Dako EnVision System, and incubated at 25˚C for 30 min. All histopathological and immunohistochemical images were captured using a Nikon ECLIPSE-CI light microscope (Nippon Kogaku) at x200 magnification. Immunohistochemistry demonstrated numerous medium-sized atypical lymphocytes proliferating in small vessel lumina, positive for B-lineage antigens (CD20, CD19 and CD79α), MUM1, BCL-2, LCA and CD5, but negative for CD3, CD10, CD23, BCL-6, TdT and CyclinD1 (Fig. 2A-P). CD34 immunohistochemical staining was positive in vascular endothelial cells, facilitating the observation of the intravascular or extravascular distribution of lymphocytes. The Ki-67 proliferation index was 80%. Immunohistochemistry demonstrated a typical pattern of intravascular tumor cell infiltration, with a small subset of lymphocytes migrating to extravascular tissues. Epstein-Barr virus-encoded RNA (EBER) detection was performed by *in situ* hybridization (ISH) using a commercial EBER probe purchased from Beijing Zhongshan Golden Bridge Biotechnology Co., Ltd. (OriGene Technologies, Inc.), with nasopharyngeal carcinoma tissue as positive control and reactive lymph node hyperplasia as negative control. The EBER ISH result was negative.

Based on these findings, the patient was ultimately diagnosed with IVLBCL of non-germinal center B-cell (non-GCB) phenotype. Minimal residual disease assessment was negative. Fluorescence *in situ* hybridization and cytogenetic studies were not performed due to the patient's refusal. Bone marrow biopsy showed mild marrow hypercellularity, a normal myeloid-to-erythroid ratio and identifiable megakaryocytes, with no definitive tumor cells identified. Immunohistochemical staining of bone marrow smears was negative for CD20 and EBER, but positive for CD61, MPO and Ki-67; occasional scattered CD3-, CD34- and CD117-positive cells were also noted (Fig. 2Q-Z). The results for MPO are not shown but are based on the pathology report.

Positron emission tomography-computed tomography (PET-CT) subsequently revealed multiple lesions with abnormally increased fluorodeoxyglucose (FDG) uptake, involving the ethmoid sinus, sphenoid sinus, bilateral CSs, right orbital mass, periaortic and pelvic lymph nodes, sacral spinal canal and left mandibular medullary cavity (Fig. 3A, C-E and I-K). The right orbital apex and periaortic lymphadenopathy showed the highest FDG uptake, with the maximum standardized uptake value (SUV_{max}) of 11.72 and 12.77, respectively. SUV_{max} values for the sphenoid sinus, bilateral CSs, sacral spinal canal

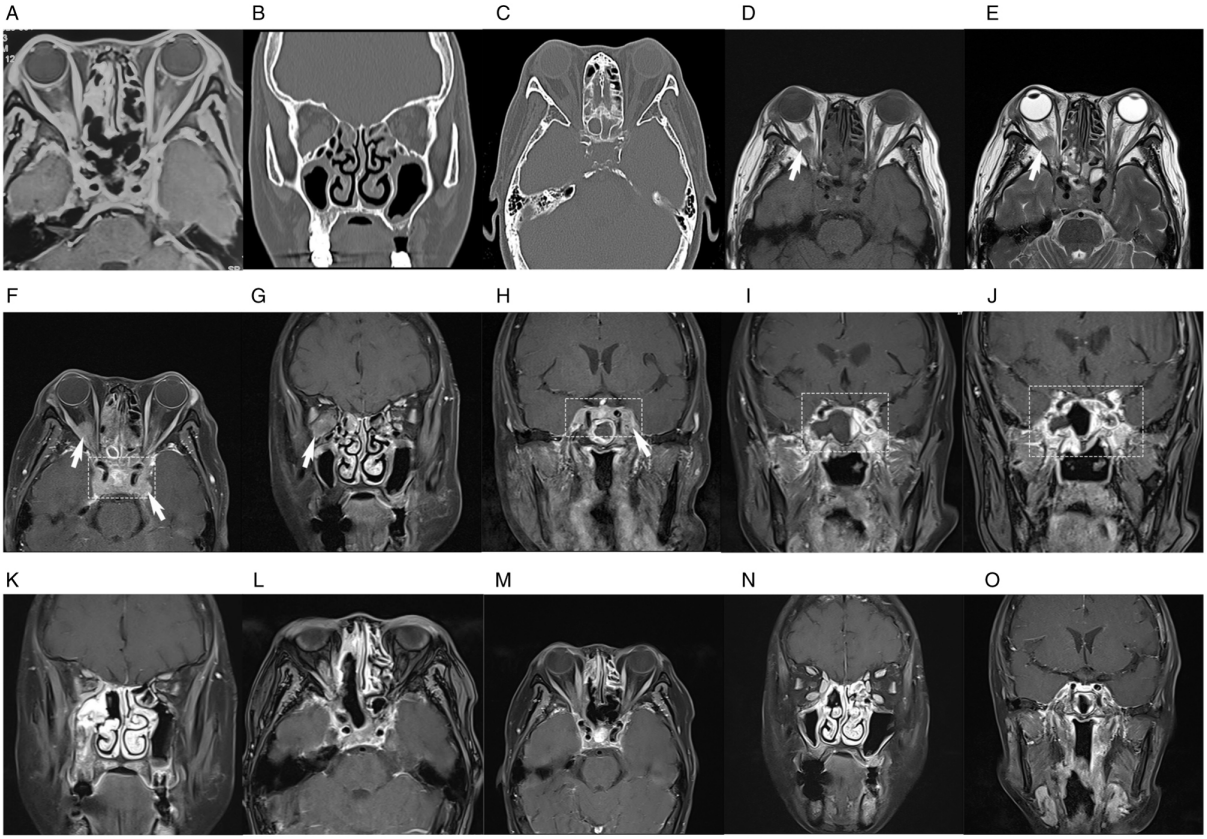

Figure 1. MRI findings and CT scan images of the patient. (A) MRI of patient at the first visit. (B) Coronal CT scan of the skull base, orbit and sinuses at the first visit. (C) Axial CT scans of the skull base, orbit and sinuses at the first visit. (D-H) Baseline MRI before initiation of the R-CHOP regimen. (D) Axial T1-weighted imaging showing a 1.2x1.6x0.9-cm lesion at the right orbital apex (white arrow). (E) Axial T2-weighted imaging. (F) Axial and (G) coronal T1 fat-suppressed gadolinium-enhanced MRI images demonstrating masses located in the right intraconal orbital space (white arrow), left intraorbital optic nerve sheaths, nasal cavity, paranasal sinuses and bilateral CSs (rectangular marquee). (H) Coronal contrast-enhanced MRI of the bilateral CSs (rectangular marquee). (I) MRI of bilateral CSs after 3 cycles of R-CHOP combined with a BTK inhibitor. (J) MRI revealing an enlarged CS lesion after 4 cycles of R-CHOP combined with a BTK inhibitor compared with that after 3 cycles of the regimen (rectangular marquee). (K) Coronal contrast-enhanced MRI of skull base, orbit and sinuses after six cycles of R-CHOP combined with BTK inhibitor and two courses of HD-MTX. (L) Axial contrast-enhanced MRI of the CS, orbit and sinuses after 6 cycles of the regimen. (M) Axial contrast-enhanced MRI of the CS, orbit and sinuses post-treatment corresponding to images F before treatment. (N) Coronal contrast-enhanced MRI of the orbit and sinuses post-treatment corresponding to images G before treatment. (O) Coronal contrast-enhanced MRI of the CS post-treatment corresponding to images H before treatment. After treatment, marked regression of the lesions in the CSs and the right orbit was observed. MRI, magnetic resonance imaging; CT, computed tomography; CS, cavernous sinus; BTK, Bruton tyrosine kinase; HD-MTX, high-dose methotrexate; R-CHOP, rituximab, cyclophosphamide, doxorubicin, vincristine and prednisolone.

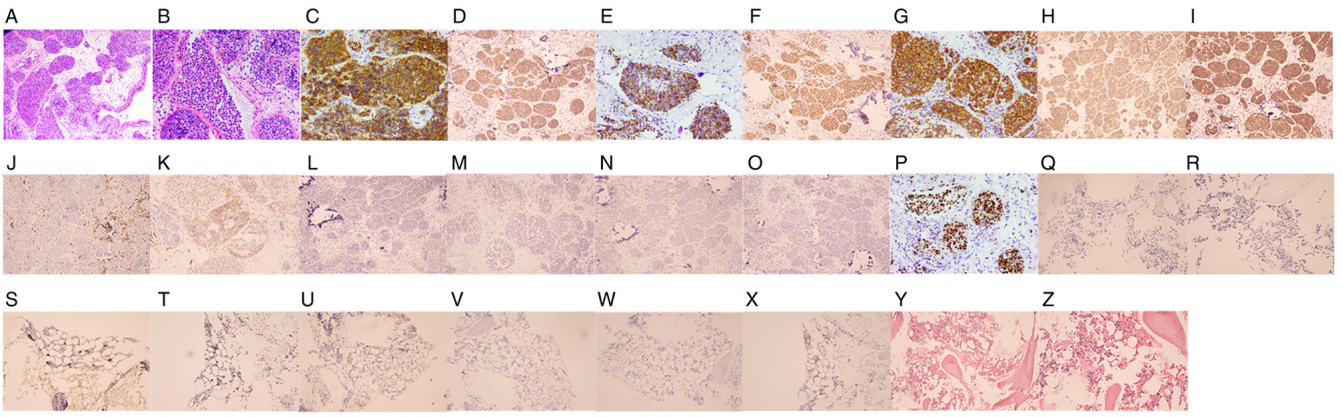

Figure 2. Histopathological findings. (A) H&E staining showing diffuse proliferation of neoplastic lymphocytes within the vascular lumina (x100 magnification). (B) H&E staining (high-power view) revealing intravascular tumor cells with marked atypia, characterized by enlarged nuclei and a high nuclear-to-cytoplasmic ratio (x400 magnification). (C-O) IHC demonstrating positive staining for (C) CD20, (D) CD19, (E) CD79α, (F) MUM1, (G) BCL-2, (H) LCA and (I) CD5 in tumor cells (x400 magnification), but negative results for (J) CD3, (K) CD10, (L) CD23, (M) BCL-6, (N) TdT and (O) cyclin D1(x400 magnification). (P) IHC staining demonstrating high tumor proliferative activity with a Ki-67 index of ~80% (x100 magnification). (Q-Z) Bone marrow biopsy. IHC staining of bone marrow smears was negative for (Q) CD20 and (R) EBER, but positive for (S) CD61 and (T) Ki67; occasional scattered (U) CD3-, (V) CD34-and (W) CD117-positive cells were also noted. (X) E-cad red-positive staining. (Y and Z) Active proliferation of bone marrow tissue, with no neoplastic cells under (Y) low- and (Z) middle-power microscopy (x200 magnification). H&E, hematoxylin and eosin; IHC, immunohistochemistry.

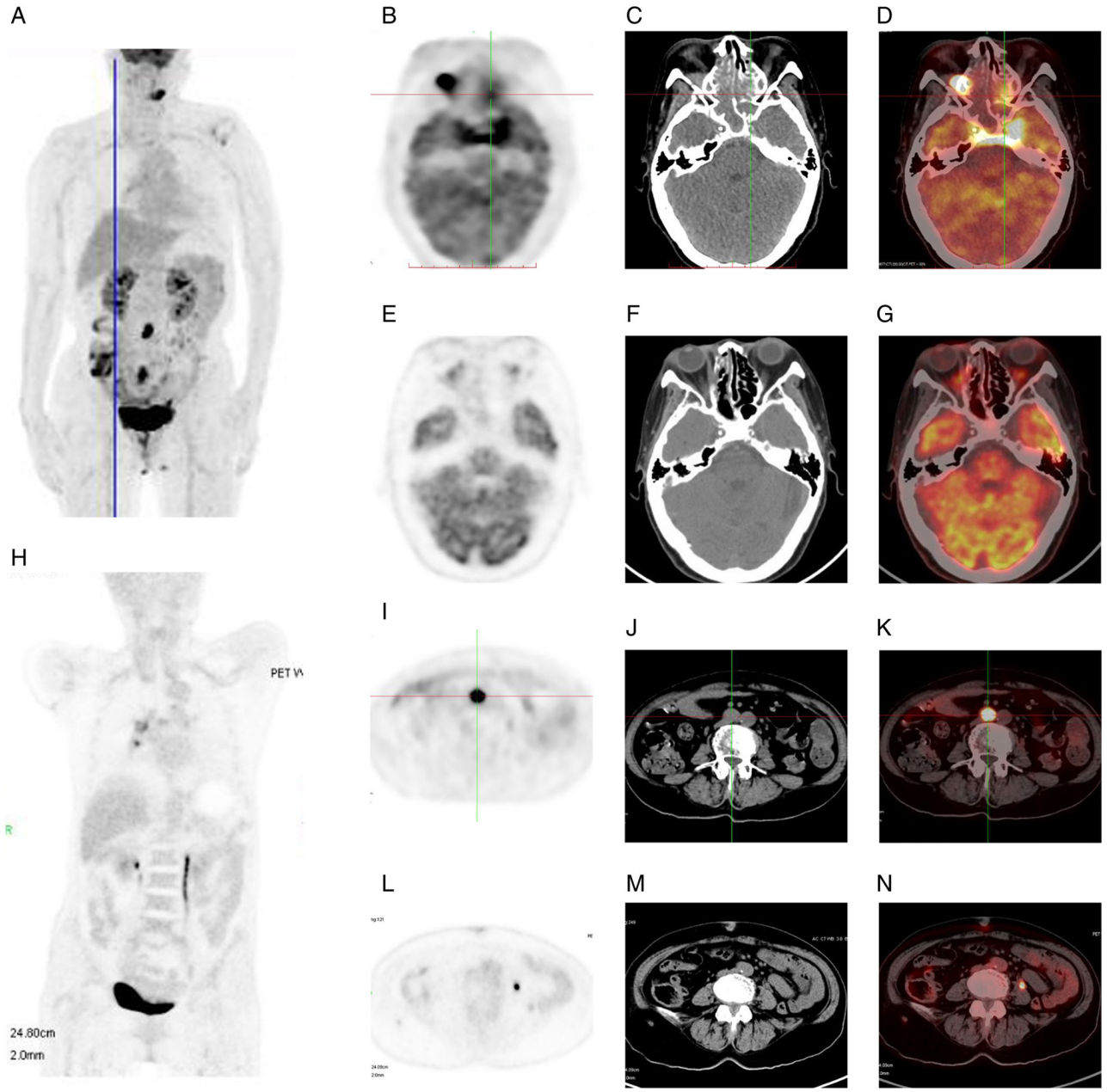

Figure 3. ^{18}F-FDG PET/CT images of the patient with intravascular large B-cell lymphoma. (A) Maximum intensity projection images at baseline. (B) Baseline PET image of the CS, orbit and sinuses. (C) Baseline CT scan image corresponding to image B. (D) Baseline PET/CT fusion image of the CS, orbit and sinuses demonstrating intense FDG uptake in the bilateral CSs and right orbital mass. (E) Follow-up PET image after treatment corresponding to image B. (F) Follow-up CT image after treatment corresponding to image C. (G) Follow-up PET/CT fusion image after treatment corresponding to image D showing complete metabolic resolution of the right orbital lesion and absence of abnormal FDG uptake in the orbit or CSs. (H) Maximum intensity projection images after eight cycles of R-CHOP regimen. (I) Baseline PET image of the abdomen. (J) Baseline CT scan image of the abdomen. (K) Baseline PET/CT fusion image of the abdomen revealing marked FDG uptake in the lymph nodes surrounding the abdominal aorta. (L) Follow-up PET image after treatment corresponding to image I. (M) Follow-up CT image after treatment corresponding to image J. (N) Follow-up PET/CT fusion image after treatment corresponding to image D demonstrating no enlarged lymph nodes or high radiotracer uptake in the abdominal cavity. (B-N) Axial view. CS, cavernous sinus; PET-CT, positron emission tomography-computed tomography; FDG, fluorodeoxyglucose; R-CHOP, rituximab, cyclophosphamide, doxorubicin, vincristine and prednisolone.

and left mandibular medullary cavity were 6.31, 9.37, 8.69 and 8.57, respectively.

Following four initial cycles of rituximab, cyclophosphamide, doxorubicin, vincristine and prednisolone (R-CHOP) (600 mg rituximab on day 0, 1 g cyclophosphamide on day 1, 100 mg doxorubicin on day 1, 4 mg vincristine on day 1, 100 mg/day prednisolone on days 0-5) combined with the Bruton tyrosine kinase (BTK) inhibitor (320 mg/day Zanubrutinib), the frontal numbness and pain of the patient was improved. However, MRI revealed an enlarged CS lesion (Fig. 1I and J), and the patient agreed to undergo high-dose methotrexate (HD-MTX) therapy (3.5 g/m^2 intravenously). After six cycles of R-CHOP combined with BTKi and two courses of HD-MTX, MRI showed a marked reduction in the CS lesion (Fig. 1K and L); however, complete remission had not yet been achieved. To further pursue complete remission, the patient agreed to receive an additional two cycles of R-CHOP. Therefore, two cycles of the same regimen (600 mg

rituximab on day 0, 1 g cyclophosphamide on day 1, 100 mg doxorubicin on day 1, 4 mg vincristine on day 1, 100 mg/day prednisolone on days 0-5 and 320 mg/day Zanubrutinib, each cycle lasting 21 days) and two courses of HD-MTX (3.5 g/m^2 intravenously) were administered. Following treatment, the diplopia, frontal numbness, bilateral ptosis and ophthalmoplegia resolved completely. Post-treatment MRI and PET-CT demonstrated marked reduction of CS enhancement and orbital mass resolution (Figs. 1M-O and 3B, F-H and L-N). Zanubrutinib (320 mg/day) was administered as maintenance therapy after chemotherapy. However, diplopia recurred again 3 months later. The patient received volumetric-modulated arc radiotherapy at 36 Gy in 18 fractions to the elective clinical target volume, including the bilateral orbits, bilateral nasal cavities, sphenoid sinus, bilateral CSs and sellar region. After completing radiotherapy, the patient declined further in-person follow-up visits. However, a recent telephone follow-up was successfully conducted at 1 year post-treatment, at which time the patient reported being alive, without ptosis and with nearly normal ocular motility.

Discussion

Current diagnostic modalities for IVLBCL, including MRI, PET-CT and plasma/CSF biomarkers, exhibit inadequate sensitivity and specificity. Histopathological biopsy thus remains the gold standard for definitive diagnosis. A previous study has advocated paranasal sinus biopsy for evaluating CS lesions (7). In the present case, transnasal endoscopic biopsy proved advantageous, offering both safety and efficiency while circumventing the substantial complications associated with craniotomy-based biopsy. Although a biopsy of the right orbital mass was deferred due to safety concerns, its consistency with a CS tumor can be reasonably inferred from characteristic MRI/PET/CT findings and a favorable clinical response to R-CHOP combined with BTKi and HD-MTX.

The underlying mechanism driving the angiotropism of neoplastic cells in IVLBCL may be associated with their immunophenotypic and molecular features. Adhesion molecules, such as CD29 and CD54, which are critical for lymphocyte trafficking and transvascular migration, have been consistently absent in IVLBCL. This deficiency likely contributes to the propensity of lymphoma cells to localize within blood vessels (8). Besides, B-cell homeostatic chemokine receptors [C-X-C chemokine receptor type 4 (CXCR4), CXCR5, C-C chemokine receptor type 6 (CCR6) and CCR7] play crucial roles in cell homing and mediate the extravascular circulation of B cells. Downregulated expression of these receptors in IVLBCL may partly explain the intravascular localization of tumor cells (9). Matrix metalloproteinases (MMPs) are key enzymes that degrade the extracellular matrix during cellular invasion and regulate blood-brain barrier (BBB) permeability under specific conditions. Notably, MMP-2 and MMP-9 are expressed in patients with primary CNS lymphoma (PCNSL) but are absent in IVLBCL cases, suggesting that MMPs may modulate the biological behavior underlying the intravascular and disseminated distribution patterns of IVLBCL (10). However, extravascular cell growth has been documented in IVLBCL cases with CNS involvement (11). Consistent with this, immunohistochemical staining in the present case displayed both intravascular and extravascular distribution.

Both the CS and orbital lesions of the present patient appeared isointense to cortical signal intensity on MRI T1- and T2-weighted images with heterogeneous enhancement. MRI findings were also consistent with an inflammatory pseudotumor, meningioma and lymphoma (12). The initial blood tests, CSF tests and peripheral blood smears revealed no evidence of a neoplasm. However, intravenous methylprednisolone pulse therapy failed to prevent disease progression, thus ruling out the diagnosis of an inflammatory pseudotumor. On MRI, meningiomas typically exhibit an isointense signal relative to gray matter on all sequences, with moderate, homogeneous contrast enhancement, and are typically accompanied by an enhancing 'dural tail' sign (13). The presence of calcifications and adjacent hyperostosis on CT is highly suggestive of meningioma (13). However, the present patient's MRI showed ill-defined lesion margins and heterogeneously enhancing lesions, with no broad-based dural attachment or enhancing 'dural tail' sign. Moreover, the CT scan demonstrated no bony destruction involving the skull base or sinuses, and no adjacent hyperostosis. The CS and orbit lesions also exhibited no calcifications on CT. Therefore, a diagnosis of meningioma was deemed unlikely. Furthermore, meningiomas that encase the cavernous internal carotid artery (ICA) often narrow its lumen, while the lesion of the present patient enlarged the CS without compressing the ICA, a feature consistent with the typical MRI findings of lymphoma (14).

Systemic lymphomas involving the orbit and skull base reported in previous studies include DLBCL, primary marginal zone BCL (MZBCL), Burkitt lymphoma (BL), mantle cell lymphoma and natural killer/T-cell lymphoma (NKTCL) (15,16). BL with involvement of the orbit, skull base and CS almost always occurs in children or young adults who are aged 2 to 39 years old (17). Furthermore, some patients with BL plus intracranial and intraorbital involvement have concurrent human immunodeficiency virus (HIV) and Epstein-Barr virus (EBV) infection (18,19). The patient in the present case was an 69-year-old woman with no evidence of HIV or EBV infection, a clinical feature distinct from that typical of BL. Patients with NKTCL plus orbital and CNS involvement exhibit characteristic MRI features typified by an abscess-like appearance on neuroimaging studies (20). This appearance arises from the angiocentric growth pattern and associated tissue destruction, which leads to zonal necrosis (20), a finding inconsistent with the MRI findings of the present patient. Mucosa-associated lymphoid tissue lymphoma, an indolent subtype of MZBCL, uncommonly involves the CNS and typically lacks any associated extracranial involvement (21). However, DLBCL and IVLBCL frequently present with multisystem involvement, with CNS involvement being a common manifestation. PET-CT confirmed that the present patient had multisystem involvement, including the CSs, a structure within the CNS. Within the literature, a previous study reported a case of adult-onset DLBCL presenting as a right CS mass extending through the superior orbital fissure and into the intraconal space of the right orbit (17). These findings were radiologically analogous to those of the present patient, yet without multisystem involvement beyond the orbit and middle cranial fossa. Therefore, it is difficult to distinguish IVLBCL

from DLBCL based on clinical and radiological manifestations alone; the gold standard for their differentiation remains pathological analysis. In previous studies, no cases of IVLBCL presenting with isolated orbital lesions have been reported; all IVLBCL patients with orbital involvement exhibit concurrent involvement of the CNS or skull base structures such as the CS (22-24). By contrast, primary orbital lesions may occur in patients with DLBCL in the absence of systemic lymphoma, and orbital manifestations may precede the diagnosis of a systemic DLBCL (15,25,26). Therefore, orbital lesions in IVLBCL are likely secondary or metastatic rather than primary in origin. Finally, the diagnosis of IVLBCL in the present case was confirmed by sphenoid sinus biopsy.

In the present case, it is hypothesized that malignant lymphocytes initially infiltrated and propagated along the vessel lumina of the left CS, leading to vascular infarction secondary to complete vessel occlusion. Subsequent ischemia and hypoxia of the cranial nerves within the CS led to the observed neurological deficits. Over time, malignant lymphocytes extended to the contralateral CS via the anterior and posterior intercavernous sinuses, causing impairments of the right cranial nerves. Histopathological analysis demonstrated that tumor cells were not strictly confined to the intravascular space, with focal extravascular infiltration observed under the microscope. This may explain the orbital involvement in this patient, with tumor cells spreading into the right orbit through the superior orbital fissure. Notably, although the patient initially presented with left-sided ocular symptoms, MRI already revealed abnormal signals in the right CS and a lesion at the right orbital apex. This clinical feature suggests that imaging changes in IVLBCL may precede clinical manifestation, possibly as the early ophthalmoplegia of the right eye was subtle and easily overlooked. Another factor is that early in the disease, multiple ocular motor cranial neuropathies in the right eye may be compressed and encased by the orbital mass, yet malignant lymphocytes primarily infiltrate the nerve sheath rather than the nerve fibers. Acute ischemia and hypoxia of these nerves, caused by intravascular lymphocyte proliferation, likely occur before compressive neuropathy. This dissociation between imaging findings and clinical symptoms indicates that even with early extravascular infiltration, IVLBCL originating from the CS may not immediately produce significant functional impairments.

IVLBCL cells display an immunophenotype consistent with mature peripheral B cells, characterized by consistent expression of pan-B-cell markers. The vast majority of cases exhibit strong CD20 expression, while CD20-negative cases typically remain positive for other pan-B-cell markers (such as CD79a and paired box protein Pax-5). According to the Hans algorithm, 82-87% of IVLBCL cases are classified as non-GCB, despite the absence of gene expression profiling in these tumors (20). Immunohistochemical analysis reveals that the expression frequencies of CD5, CD10, BCL6 and MUM1 are 22-75, 13-22, 22-26 and 75-80%, respectively (16). Despite variable frequencies, none of these markers correlate with prognostic differences (27,28). Previous research has shown that CD5(+)/CD10(-) IVLBCL is correlated with a higher incidence of thrombocytopenia and bone marrow/peripheral blood involvement, but a lower rate of neurological abnormalities compared with the CD5(-)/CD10(-) subtype (29). No significant differences were observed in other clinical features or survival outcomes between the two subtypes (29). Notably, the present case, displaying a CD5(+)/CD10(-) immunophenotype, presented with neurological manifestations such as cranial nerve palsies, underscoring the need for further studies on the heterogeneity of clinical presentation and immunophenotype in IVLBCL.

IVLBCL is a rare malignancy with no established standard treatment. Although the R-CHOP regimen has been shown to significantly improve survival rates in IVLBCL patients, the prognosis remains guarded, particularly in those with CNS involvement (30,31). In CNS-involved IVLBCL, 1- and 2-year overall survival rates were 44.2 and 22.2%, respectively, with treatment approaches varying across HD-MTX plus R-CHOP, MTX, cytarabine and intrathecal MTX (1). Notably, BTKis, which can block the NF-κB pathway and penetrate the BBB, have shown promising outcomes in patients with IVLBCL and CNS involvement (31). Previous studies have reported frequent mutations in NF-κB pathway genes in IVLBCL and a substantial number of CNS-involved patients sensitive to treatment with BTKis (31,32). Notably, zanubrutinib, a selective BTKi, in combination with R-CHOP, achieved complete responses in all patients, including those with CNS involvement (1). Additionally, a patient with primary CNS lymphoma, who could not tolerate intensive therapy or undergo consolidative autologous stem cell transplant (ASCT) or whole-brain radiotherapy, remained in remission for 18 months while undergoing monotherapy with acalabrutinib, a BTKi (33). Although no standard consolidation or maintenance strategy has been established for conventional BCL with CNS involvement, accumulating evidence indicates that BTKis demonstrate favorable efficacy and tolerability in highly aggressive lymphomas with a high risk of relapse, such as IVLBCL and PCNSL, particularly in elderly patients or those ineligible for ASCT (31,33-37). Therefore, maintenance therapy with zanubrutinib was initiated for the present patient after obtaining informed consent.

In the present case, four initial cycles of R-CHOP combined with BTKi therapy yielded poor efficacy, suggesting that the R-CHOP regimen may not be an effective induction regimen for IVLBCL with CS involvement. Although R-CHOP demonstrates efficacy in systemic DLBCL, its outcomes remain suboptimal in cases with CNS involvement (38). Key drugs of the R-CHOP regimen, including vincristine and doxorubicin, as well as the large monoclonal antibody rituximab, exhibit limited permeability across the BBB and blood-CSF barrier, leading to inadequate drug exposure at skull base structures such as the CS. Besides, BTKis generally demonstrate limited BBB penetration. Zanubrutinib, a second-generation BTKi, has improved BBB permeability compared with first-generation agents; however, its efficacy may be restricted in IVLBCL cases that are not dependent on the BCR/NF-κB signaling pathway (31). Furthermore, immune escape and immune privilege may lead to the limited efficacy of R-CHOP. However, in the present study, following two courses of HD-MTX, a marked reduction in the size of the CS lesion was observed, highlighting the critical role of BBB-penetrating agents in disease control. Accordingly, for patients with IVLBCL plus orbit and CS

involvement, a treatment strategy combining R-CHOP with BBB-penetrating agents such as HD-MTX may be more appropriate. In the present patient, maintenance therapy with a BTKi was not effective. These findings highlight the need to explore individualized chemotherapy regimens for patients with IVLBCL plus CNS and skull base involvement, as well as to develop more targeted therapeutic strategies employing BBB-penetrating agents.

A previous study reported comparable rates of CNS relapse in patients with DLBCL treated with HD-MTX and those receiving intrathecal MTX (IT-MTX) (39). In a cohort of 88 patients with aggressive BCL involving extralymphatic craniofacial sites, the 2-year rate of CNS disease was 4.2% among 88 patients who received IT-MTX prophylaxis, compared with 2.3% among 191 patients who did not (40). Moreover, a matched case-control retrospective study of patients with PCNSL treated with HD-MTX, with or without adjunctive IT-MTX, demonstrated no significant difference in survival, disease control or neurotoxicity between the two groups (41). Therefore, IT-MTX does not confer superiority over HD-MTX in either the treatment or prevention of BCL with CNS and skull involvement. In addition, an increasing number of case reports have described adverse effects associated with IT-MTX, including myelopathy and severe neurological complications (42,43). Given the absence of abnormalities on CSF examination in the present patient, HD-MTX monotherapy was selected rather than combination therapy with IT-MTX.

In conclusion, IVLBCL is often misdiagnosed as an inflammatory disorder, but the diagnosis should be considered when patients sequentially develop CS syndrome, fail to respond to steroid therapy, and particularly exhibit a dissociation between imaging findings and clinical manifestations. A prompt biopsy is essential to establish a definitive diagnosis. BTKi therapy in combination with HD-MTX plus R-CHOP may provide an effective therapeutic strategy for controlling IVLBCL with skull base and orbital involvement. Nevertheless, more effective maintenance or consolidation treatment strategies should be actively explored.

Acknowledgements

Not applicable.

Funding

Funding was provided by the Natural Science Foundation of China (grant no. 82205194).

Availability of data and materials

The data generated in the present study may be requested from the corresponding author.

Authors' contributions

QW and LBJ conceived and designed the study, and contributed to manuscript drafting. BY and YJ collected and analyzed the MRI and CT images from the patient records, interpreted the radiological findings and contributed to the discussion of imaging characteristics in the manuscript. XH performed the histological examination of the tumor, including IHC staining and ISH assays, and contributed to the pathological diagnosis. HL was involved in revising the manuscript for important intellectual content, critically reviewed the pathological and radiological data, and provided clinical guidance for the study design and patient management. All authors have read and approved the final version of the manuscript. QW and LBJ have checked and confirmed the authenticity and integrity of all raw data.

Ethics approval and consent to participate

This study was conducted in accordance with the principles expressed in the Declaration of Helsinki.

Patient consent for publication

Written and verbal consent was obtained from the patient for publication of the case report and any accompanying images.

Competing interests

The authors declare that they have no competing interests.

References

1. Li Y, Li S, Liu X, Xue W, Han L, Li Y, Zhang X and Zhang M: Clinical features and prognostic factors of intravascular large B-cell lymphoma: A cohort study of 20 patients from 2018 to 2024. Oncologist 30: oyaf156, 2025.
2. Rajyaguru DJ, Bhaskar C, Borgert AJ, Smith A and Parsons B: Intravascular large B-cell lymphoma in the United States (US): A population-based study using Surveillance, epidemiology, and end results program and National cancer database. Leuk Lymphoma 58: 1-9, 2017.
3. Geer M, Roberts E, Shango M, Till BG, Smith SD, Abbas H, Hill BT, Kaplan J, Barr PM, Caimi P, *et al*: Multicentre retrospective study of intravascular large B-cell lymphoma treated at academic institutions within the United States. Br J Haematol 186: 255-262, 2019.
4. Kim TR, Bae KN, Son JH, Shin K, Kim H, Ko H, Kim B and Kim MB: A case of cavernous sinus Syndrome due to extranodal diffuse large B-cell lymphoma. Ann Dermatol 35 (Suppl 2): S300-S303, 2023.
5. Wang D, Marous CL, Ozay F, Timashpolsky A, Gulati RD, Gottesman SRS, Boruk M, Shinder R and Hodgson NM: Intravascular large B-cell lymphoma diagnosed by nasal biopsy in a patient presenting with bilateral ptosis and ophthalmoplegia. Orbit 42: 450-454, 2023.
6. Jain R, Sawhney S, Koul RL and Chand P: Tolosa-Hunt syndrome: MRI appearances. J Med Imaging Radiat Oncol 52: 447-451, 2008.
7. Zhang AS, Jonker BP, Morris CL, Campbell RG, Alvarado R, Winder M, Sacks R, Seresirikachorn K and Harvey RJ: Endoscopic endonasal biopsy for diagnosis of undifferentiated lesions of the cavernous sinus. World Neurosurg 175: e391-e396, 2023.
8. Ponzoni M, Arrigoni G, Gould VE, Del Curto B, Maggioni M, Scapinello A, Paolino S, Cassisa A and Patriarca C: Lack of CD 29 (beta1 integrin) and CD 54 (ICAM-1) adhesion molecules in intravascular lymphomatosis. Hum Pathol 31: 220-226, 2000.
9. Kasuya A, Fujiyama T, Shirahama S, Hashizume H and Tokura Y: Decreased expression of homeostatic chemokine receptors in intravascular large B-cell lymphoma. Eur J Dermatol 22: 272-273, 2012.
10. Kinoshita M, Izumoto S, Hashimoto N, Kishima H, Kagawa N, Hashiba T, Chiba Y and Yoshimine T: Immunohistochemical analysis of adhesion molecules and matrix metalloproteinases in malignant CNS lymphomas: A study comparing primary CNS malignant and CNS intravascular lymphomas. Brain Tumor Pathol 25: 73-78, 2008.

11. Poropatich K, Dittmann D, Chen YH, Raparia K, Wolniak K and Gao J: A small case series of intravascular large B-cell lymphoma with unexpected findings: Subset of cases with concomitant extravascular central nervous system (CNS) involvement mimicking primary CNS lymphoma. J Pathol Transl Med 51: 284-291, 2017.
12. Jacobs D and Galetta S: Diagnosis and management of orbital pseudotumor. Curr Opin Ophthalmol 13: 347-351, 2002.
13. Bonneville F, Jäger HR and Smirniotopoulos JG: Differential diagnosis of intracranial masses. In: Diseases of the Brain, Head and Neck, Spine 2024-2027: Diagnostic Imaging. Chapter 8. Hodler J, Kubik-Huch RA and Roos JE (eds). Springer, Cham, CH, 2024.
14. Munawar K, Nayak G, Fatterpekar GM, Sen C, Zagzag D, Zan E and Hagiwara M: Cavernous sinus lesions. Clin Imaging 68: 71-89, 2020.
15. Fritzhand SJ, Esmaeli B, Sun J and Debnam JM: Primary disease sites and patterns of spread in cases of neurolymphomatosis in the orbit associated with lymphoma. Cancer Imaging 21: 39, 2021.
16. Choi HK, Cheon JE, Kim IO, Youn BJ, Jung AY, Shin SM, Kim WS and Yeon KM: Central skull base lymphoma in children: MR and CT features. Pediatr Radiol 38: 863-867, 2008.
17. Ko F and Subramanian PS: Orbital and cavernous sinus lymphoma masquerading as post-herpetic neuralgia. Neuroophthalmology 35: 27-31, 2011.
18. Ruiz-Ortiz M, Azcarate-Diaz FJ, Galindo-Rodriguez D, Torres-Calcines N and Calleja-Castano P: Cavernous sinus syndrome as the initial symptom of Burkitt's lymphoma: A case report and literature review. Rev Neurol 69: 249-254, 2019 (In Spanish).
19. Reyneke F, Mokgoro N, Vorster M and Sathekge M: Burkitt lymphoma and cavernous sinus syndrome with breast uptake on 18F-FDG-PET/CT: A case report. Medicine (Baltimore) 96: e8687, 2017.
20. Chen CS, Miller NR, Lane A and Eberhart C: Third cranial nerve palsy caused by intracranial extension of a sino-orbital natural killer T-cell lymphoma. J Neuroophthalmol 28: 31-35, 2008.
21. Yang CC, Chen TY, Tsui YK and Ko CC: Primary marginal zone B-cell lymphoma of the cavernous sinus: A case report and review of the literature. BMC Med Imaging 21: 25, 2021.
22. Roditi E, Panicker S and Fung AT: Intravascular large B-cell lymphoma of the eye: Literature review and new findings. Asia Pac J Ophthalmol (Phila) 13: 100053, 2024.
23. Berbos ZJ, Lee MS, Zaldivar RA, Pambuccian S and Harrison AR: Intravascular lymphoma presenting as an orbital mass lesion: A case report. Orbit 29: 91-93, 2010.
24. Sato T, Goto H, Toratani A, Yamagata N, Ashihara E, Oku N, Inaba T, Fujita N, Shimazaki C and Nakagawa M: Neoplastic angioendotheliosis presenting Tolosa-Hunt syndrome, intraspinal invasion and intraorbital tumor. Rinsho Ketsueki 35: 557-561, 1994 (In Japanese).
25. Singh S and Ali MJ: Lymphoproliferative tumors involving the lacrimal drainage system: A major review. Orbit 39: 276-284, 2020.
26. Liu H, Ren YJ, Chen YM, Yang JR, Yang J, Cai FM, Lei T and Liu HL: Clinical and histopathological characteristics of 19 cases of orbital diffuse large B-cell lymphoma. Zhonghua Yan Ke Za Zhi 62: 52-58, 2026 (Chinese).
27. Della Mura M, Sorino J, Angiuli FE, Cazzato G, Gaudio F and Ingravallo G: Intravascular lymphoma: A unique pattern underlying a protean disease. Cancers (Basel) 17: 2355, 2025.
28. Ponzoni M, Campo E and Nakamura S: Intravascular large B-cell lymphoma: A chameleon with multiple faces and many masks. Blood 132: 1561-1567, 2018.
29. Murase T, Yamaguchi M, Suzuki R, Okamoto M, Sato Y, Tamaru J, Kojima M, Miura I, Mori N, Yoshino T and Nakamura S: Intravascular large B-cell lymphoma (IVLBCL): A clinicopathologic study of 96 cases with special reference to the immunophenotypic heterogeneity of CD5. Blood 109: 478-485, 2007.
30. Seegobin K, Li Z, Alhaj Moustafa M, Majeed U, Wang J, Jiang L, Kuhlman J, Menke D, Li K, Kharfan-Dabaja MA, *et al*: Clinical characteristics, prognostic indicators, and survival outcomes in intravascular lymphoma: Mayo Clinic experience (2003-2018). Am J Hematol 97: 1150-1158, 2022.
31. Shao F, Su W, Zhao X, He J, Wang X, Guo F and Xiao H: Successful treatment of hemophagocytic intravascular large B-cell lymphoma with CNS involvement with BTK inhibitor combined with rituximab and high-dose methotrexate. Ther Adv Hematol 15: 20406207241270788, 2024.
32. Schrader AMR, Jansen PM, Willemze R, Vermeer MH, Cleton-Jansen AM, Somers SF, Veelken H, van Eijk R, Kraan W, Kersten MJ, *et al*: High prevalence of MYD88 and CD79B mutations in intravascular large B-cell lymphoma. Blood 131: 2086-2089, 2018.
33. Allison E, Campbell A, Watson AM and Beaton B: Acalabrutinib may offer a new therapeutic approach for consolidation and maintenance of primary CNS lymphoma with expression of MYD88 and CD79B gene variants: A case report and literature review of primary CNS lymphoma in the BTKi Era. Int J Mol Sci 26: 10521, 2025.
34. Yu L, Ping N, Zou R, Zhu Q, Li J, Zhang X, Xia F, He J, Tu J, Kong D, *et al*: Sustained remission with PD-1 and BTK inhibitors maintenance after chimeric antigen receptor T-cell therapy in CNS lymphoma. Cancer Immunol Immunother 74: 372, 2025.
35. Du S, Bota D and Kong XT: Successful consolidation/maintenance therapy with single agent ibrutinib for primary CNS lymphoma after initial induction therapy. Neurol Int 14: 574-580, 2022.
36. Du S, Fu DB, Bota D and Kong XT: Prolonged remission with ibrutinib maintenance therapy following radiation in a patient with relapsed primary CNS lymphoma. CNS Oncol 13: 2345579, 2024.
37. Cheng CL, Yuan CT, Fang WQ, Huang PH, Hou HA, Tsai CH, Yao M, Chou WC and Tien HF: Both consolidation and maintenance treatment improve outcomes in primary central nervous system lymphoma: Real-world evidence from a tertiary medical center. J Cancer 16: 1836-1847, 2025.
38. Nayak L and Batchelor TT: Is it time to revisit R-CHOP for primary CNS lymphoma? Blood 134: 221-222, 2019.
39. Akimoto M, Miyazaki T, Takahashi H, Saigusa Y, Takeda T, Hibino Y, Tokunaga M, Ohashi T, Matsumura A, Teshigawara H, *et al*: Comparison of standardized prophylactic high-dose and intrathecal methotrexate for DLBCL with a high risk of CNS relapse. Int J Hematol 119: 164-172, 2024.
40. Murawski N, Held G, Ziepert M, Kempf B, Viardot A, Hänel M, Witzens-Harig M, Mahlberg R, Rübe C, Fleckenstein J, *et al*: The role of radiotherapy and intrathecal CNS prophylaxis in extralymphatic craniofacial aggressive B-cell lymphomas. Blood 124: 720-728, 2014.
41. Khan RB, Shi W, Thaler HT, DeAngelis LM and Abrey LE: Is intrathecal methotrexate necessary in the treatment of primary CNS lymphoma? J Neurooncol 58: 175-178, 2002.
42. Nelson RW and Frank JT: Intrathecal methotrexate-induced neurotoxicities. Am J Hosp Pharm 38: 65-68, 1981.
43. Rodrigues PGB, Lima TT, Duarte FB and Nóbrega PR: Myelopathy associated with intrathecal methotrexate. Pract Neurol 22: 141-144, 2022.